Bioorganic & Medicinal Chemistry 16 (2008) 7134–7140

Contents lists available at ScienceDirect

Bioorganic & Medicinal Chemistry

journal homepage: www.elsevier.com/locate/bmc

# QSAR study of imidazoline antihypertensive drugs

Katarina Nikolic *, Slavica Filipic, Danica Agbaba

*Institute of Pharmaceutical Chemistry and Drug Analysis, Faculty of Pharmacy, University of Belgrade, Vojvode Stepe 450, 11000 Belgrade, Serbia*

ARTICLE INFO

*Article history:*
Received 15 May 2008
Revised 19 June 2008
Accepted 26 June 2008
Available online 28 June 2008

*Keywords:*
$I_1$-receptor
$I_1$-R ligands
Centrally acting antihypertensives
Structure–activity relationship
Pharmacophore

ABSTRACT

The hypotensive effect of imidazoline ligands was attributed to both $\alpha_2$-adrenergic receptors and nonadrenergic imidazoline-1 receptors ($I_1$-R). Selective $I_1$-R ligands, devoid of the typical side effects of other centrally acting antihypertensive drugs, could be widely used in antihypertensive therapy. Thus, there is significant interest in developing new imidazoline analogs with higher selectivity and affinity for $I_1$ receptors. The quantitative structure–activity relationship (QSAR) study of 12 ligands was carried out using multilinear regression method on $I_1$-R and $\alpha_2$-adrenergic receptors binding affinities on human platelets. The compounds have been studied using Becke3LYP/3-21G (d,p) and Becke3LYP/6-31G(d,p) DFT methods. Among 42 descriptors that were considered in generating the QSAR model, three descriptors such as partial atomic charges of nitrogen in the heterocyclic moiety, distribution coefficient, and molar refractivity of the ligands resulted in a statistically significant model with $R^2 = 0.935$ and cross-validation parameter $q^2_{pre} = 0.803$. The validation of the QSAR models was done by cross-validation and external test set prediction. The developed multiple linear regression models for the $I_1$-R ligands were aimed to link the structures to their reported $I_1$-R binding affinity $\log(1/K_i)$. The theoretical approach indicates that an increase in distribution coefficient and molar refractivity value, together with a decrease in average N-charge in the heterocyclic moiety of the ligands, causes better binding affinity for active site of the $I_1$ receptors. The developed QSAR model is intended to predict $I_1$-R binding affinity of related compounds and to define possible physicochemical, electronical, and structural requirements for selective $I_1$-receptor ligands.



## 1. Introduction

The hypotensive effect of imidazoline ligands was attributed to both $\alpha_2$-adrenergic receptors ($\alpha_2$-AR) and nonadrenergic imidazoline-1 receptors ($I_1$-R).[1] Therefore, both $\alpha_2$-AR agonists and $I_1$-R agonists are capable of lowering sympathetic tone by a primary action in the rostral ventrolateral medulla (RVLM). The $\alpha_2$-AR agonists directly inhibit presympathetic RVLM neurons. The $I_1$-R agonists increase the release of catecholamines in the RVLM, and the catecholamines, in turn, depress presympathetic RVLM neurons by activating $\alpha_2$-AR.[2–4]

According to the imidazoline hypothesis, imidazoline $I_1$ receptors in the RVLM are important for the sympathoinhibitory action of clonidine, and the role of $I_1$ receptors ($I_1$-R) is particularly prominent in the case of rilmenidine and moxonidine.

The antihypertensive ligands moxonidine and rilmenidine showed higher affinity for $I_1$-imidazoline sites than for $\alpha_2$-AR, as well as higher selectivity for $I_1$ imidazoline sites than clonidine.[2–4] Rilmenidine and moxonidine cause only few $\alpha_2$-adrenoceptor-mediated side effects because they are selective for $I_1$ receptors.

Further pharmacological studies will need to elucidate the close interdependence and interaction of these two receptors at the cellular level, and to explain their complex role in the central hypotensive effect of the ligands.

Specific imidazoline receptors ($I_1$-R, $I_2$-R, and $I_3$-R) have been characterized by extensive biochemical and physiological studies.[1,5] The subcellular localization of $I_1$-R to the plasma membrane has been assessed in the bovine brainstem,[6,7] in the human platelets, [8] and in the PC12 cells.[9,10]

The $I_1$-R protein structures have not yet been solved to date. Only imidazoline receptor antisera-selected (IRAS) gene candidate for the $I_1$-R protein has been proposed.[11–13] Since the imidazoline binding site may only be formed when IRAS-1 is complexed to the fibronectin receptor or other partner proteins,[14] characterization of $I_1$ ligand–IRAS-1 complexes requires special experimental procedure. Therefore, quantitative structure–activity relationship (QSAR) study could be reliable tool for examination of the $I_1$-R ligands.

Previous quantum chemical studies have been restricted to similar systems (cyclic imidazolines, oxazolines, and thiazolines).[15–17] These theoretical studies set out to determine stable conformations, tautomeric equilibria, gas-phase reactivity, and lipophilicity of clonidine and rilmenidine.[15] Previously determined crystal

* Corresponding author. Tel.: +381 63 84 30 677.
*E-mail address:* knikolic@pharmacy.bg.ac.yu (K. Nikolic).

0968-0896/$ - see front matter © 2008 Elsevier Ltd. All rights reserved.
doi:10.1016/j.bmc.2008.06.051

structures of clonidine hydrochloride[18] and rilmenidine phosphate[19] were used as reference values for geometric parameters of the real systems.

Here, we present a quantitative structure–activity relationship (QSAR) study designed to rationalize the relationship between the structural and physicochemical features of a series of 12 imidazoline/oxazoline/guanidine analogs and their binding affinities to $I_1$, $\alpha_{2A}$, $\alpha_{2A}$, and $\alpha_{2A}$ receptors on human platelets.[20]

The derived $K_i$ values for the 12 ligands at the human platelet $I_1$ site, generated under a 10 μM (−) norepinephrine (NE) mask, were collected from literature.[20] Very low affinity of NE ($K_i$, 1 mM) for platelet $I_1$-imidazoline sites and high affinity for $\alpha_2$-AR provide selective masking of $\alpha_2$-binding sites in platelet membranes.[7] The compounds were selected with an intention of covering a wide range of $I_1$-R affinities, and the negative logarithm of their $K_i$, that is, ($pK_i$) values was calculated.

Higher $I_1/\alpha_2$ receptor selectivity of centrally acting antihypertensives greatly reduces the adverse effects attributable to dominant stimulation of $\alpha_2$-adrenoceptors, observed with the first generation of centrally acting agents.[7] Therefore, the QSAR study of $I_1$-R ligands in combination with QSAR study of their $I_1/\alpha_2$-selectivity can be very helpful in activity evaluation of other related centrally acting antihypertensives.

## 2. Calculation

The $I_1$-R affinities ($K_i$) of 12 $I_1$-ligands, measured on human platelets plasma membranes under a 10-μM (−) norepinephrine (NE) mask, were collected from literature.[20] The ligands for the QSAR study were selected with an intention of covering a wide range of $I_1$-R affinities, and the negative logarithm of their $K_i$, that is, ($pK_i$) values was calculated.

The pKa calculation and selection of dominant molecules/cations at physiological pH 7.4, were performed for the examined $I_1$-R ligands using the Marvin 4.0.5 ChemAxon program.[21] The computer program Marvin 4.0.5 uses computational algorithms based on the fundamental chemical structure theory to estimate a variety of chemical reactivity parameters.

The geometries of the examined ligands (**1**–**12**, **T1**, **T2**, Figs. 1 and 3) were completely optimized at B3LYP/3–21(d,p) levels of the density functional theory[22,23] using the Gaussian 98 program.[24]

The CS Gaussian 98 program[24] using the B3LYP hybrid functional including 6-31G(d,p) basis set with Polarizable Continuum Model (PCM) in water solution,[25,26] was applied for molecular parameters computation of the optimized models.

The selected Gaussian basis set methods for examination of the molecules have proven to be a very good choice to predict the molecular parameters of related aromatic and organic compounds.[15–17]

Furthermore, the partition coefficient octanol/water (log*P*), $pK_a$, distribution coefficient (log*D*), isoelectric point, total charge, Connolly solvent accessible surface area (SAS), Connolly molecular surface area (MS), molar refractivity (MR), and polar surface area (PSA) were determined by use of the ChemProp[27] and ChemAxon Marvin 4.0.5 programs.[21]

Structure of the $I_1$-R active site was optimized by molecular mechanics, using the UFF method[28] implemented in Argus Lab 4.0.1 (Planaria Software).[29]

Amino acid sequence of active domain of the $I_1$-R (NCBI locus: AAC33104)[30] wase obtained from National Center for Biotechnology Information Database (www.ncbi.nlm.nih.gov). Flexible ligand docking was performed with help of Argus Lab 4.0.1.[29] Optimized docking conformations of the ligands at the $I_1$-R active site were examined.

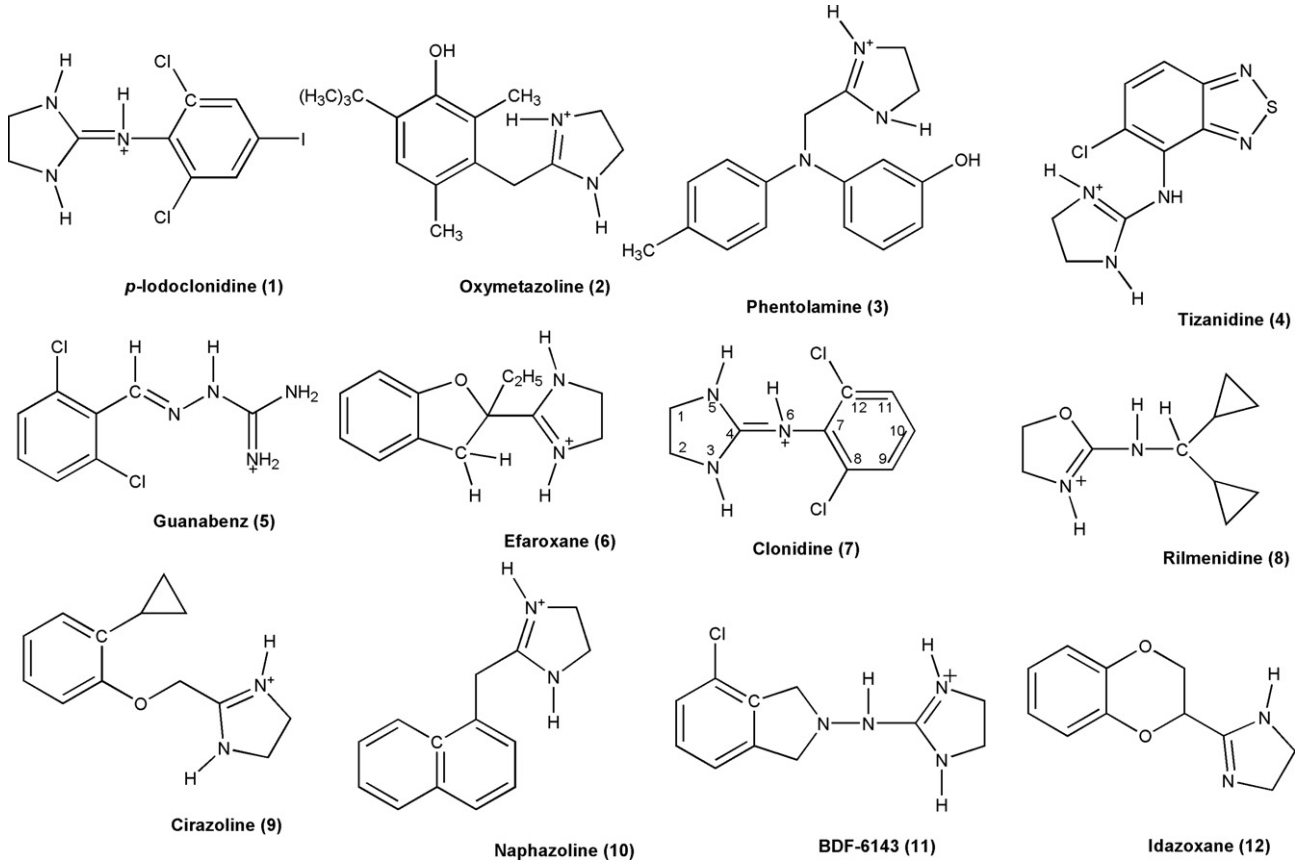


**Figure 1.** Structural formulas of $I_1$-R ligands used for the QSAR study. The depicted structures are the most dominant forms of the compounds at pH 7.4 (Marvin 4.0.5 ChemAxon).

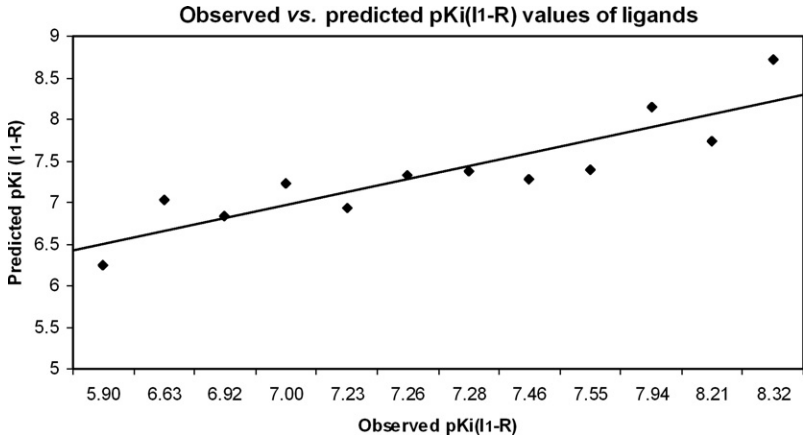


**Figure 2.** Plot of observed vs. predicted pKi($I_1$-R) values of $I_1$-R ligands (**1**–**12**). Predicted p$K_i$($I_1$-R) values are from cross-validation process.

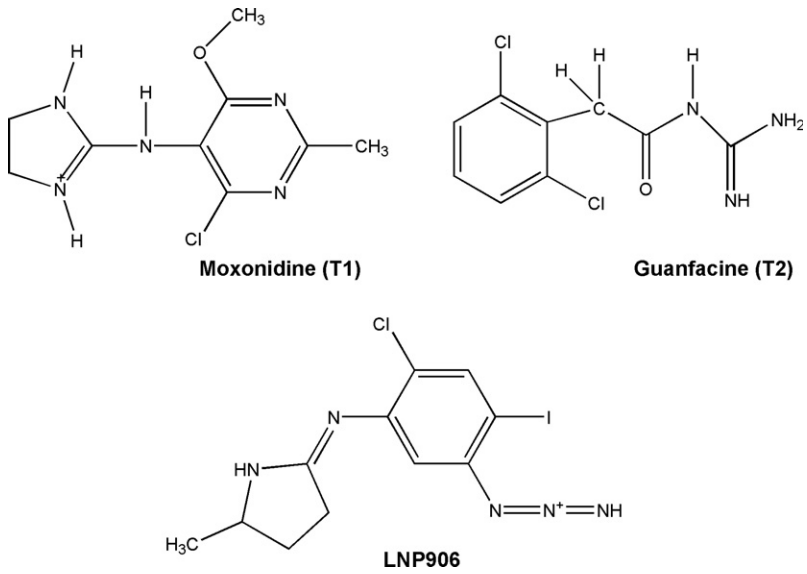


**Figure 3.** Structural formulas of moxonidine (T1), guanfacine (T2), and LNP906 that are used for external test of the QSAR model. The depicted structures are the most dominant forms of the compounds at pH 7.4 (Marvin 4.0.5 ChemAxon).

A preliminary data analysis showed a good spread and distribution of the p$K_i$ ($I_1$) values (Table 1), which spanned about a 3 log unit range (from 5.90 to 8.32). This was a good precondition for the derivation of meaningful models. Single and multivariable linear regression models were developed for the data set by use of the Microsoft-Excel 2000/Regression Data Analysis and Multi-precision Floating Point Computation for Excel (XNUMBERS.XLA-Ver.4.7-2006).[31]

In our study, 42 various physicochemicals, topological, and electrostatic descriptors were evaluated in terms of their efficacy to predict the $I_1$-R and $\alpha_2$-AR binding affinity and $I_1$-R/$\alpha_2$-AR selectivity. The correlation coefficients for all calculated molecular parameters with experimentally determined $I_1$-R affinities (p$K_i$ ($I_1$-R)) $\alpha_2$-AR binding affinity (p$K_i$ ($\alpha_2$-AR)) and $I_1$-R/$\alpha_2$-AR selectivity (p$K_i$ $I_1$-R)-p$K_i$($\alpha_2$-AR))[20] were determined. The molecular properties with the highest correlation coefficients (correlation factor $r \geqslant 0.55$) were selected for multilinear regression study. Inter-correlation between these descriptors was checked for independence of the variables. The optimum number of components (latent variables) is determined by multilinear correlation coefficients, and the model predictive ability is assessed by cross-validation $r^2(r^2_{cv}, q^2)$ and external test set prediction (RMSEE).[32]

**Table 1**
Experimental and computed geometry of clonidine hydrochloride

| Parameter[a] | Clonidine hydrochloride [a] | | | |
|---|---|---|---|---|
| | X-ray[18] | B3LYP/ 6-31+(d,p)[17] | BP86/ TZ2P–CPCM[17] | B3LYP/ 3-21(d,p) |
| *d*[C(1)–N(5)] | 1.447 | 1.478 | 1.478 | 1.497 |
| *d*[C(1)–C(2)] | 1.532 | 1.546 | 1.550 | 1.572 |
| *d*[N(5)–C(4)] | 1.321 | 1.373 | 1.387 | 1.340 |
| *d*[C(4)–N(3)] | 1.322 | 1.307 | 1.294 | 1.343 |
| *d*[N(3)–C(2)] | 1.450 | 1.469 | 1.472 | 1.500 |
| *d*[C(4)–N(6)] | 1.327 | 1.355 | 1.377 | 1.343 |
| *d*[N(6)–C(7)] | 1.418 | 1.423 | 1.411 | 1.437 |
| Θ[C(1)–N(5)–C(4)] | 111.4 | 107.7 | 106.5 | 111.6 |
| Θ[N(5)–C(4)–N(3)] | 111.7 | 113.3 | 115.7 | 111.3 |
| Θ[N(5)–C(1)–C(2)] | 102.6 | 101.8 | 101.7 | 101.9 |
| Θ[C(4)–N(3)–C(2)] | 110.6 | 109.6 | 107.8 | 111.4 |
| Θ[C(1)–C(2)–N(3)] | 103.5 | 103.9 | 104.9 | 101.9 |
| Θ[N(5)–C(4)–N(6)] | 123.1 | 120.2 | 117.2 | 124.1 |
| Θ[C(4)–N(6)–C(7)] | 123.0 | 123.9 | 124.4 | 122.3 |
| Φ[C(1)–N(5)–C(4)–N(3)] | 1.0 | −11.2 | −11.7 | −4.9 |
| Φ[N(5)–C(4)–N(3)–C(2)] | −0.5 | −2.8 | 0.2 | −4.3 |
| Φ[N(5)–C(1)–C(2)–N(3)] | 0.7 | −19.9 | −16.6 | −12.4 |
| Φ[C(1)–N(5)–C(4)–N(6)] | −177.3 | 168.8 | 169.4 | 175.2 |
| Φ[C(4)–N(6)–C(7)–C(8)] | −76.4 | −106.6 | −118.5 | −94.9 |

[a] For numbering of atoms, see Figure 1.

The quality of the regression fits was estimated using parameters such as the regression factor ($r$), square of regression factor ($R^2$), adjusted square of regression factor ($R^2_{adj}$), $q^2_{pre}$ (validation $R^2$), $F$ ratio, and $P$ values,[32] which are defined below

$$R^2 = \frac{SSTo - SSE}{SSTo} \quad (1)$$

$$R^2_{adj} = 1 - \frac{MSE}{MS(Total)} \quad (2)$$

The $R^2$ and $R^2_{adj}$ parameters indicate how closely the regression function fits the given values of $y_{data,i}$. Variation, sum of squares (Total)

$$SSTo = \sum_{i=1}^{n} (y_{data,i} - \bar{y})^2 \quad (3)$$

Variation, sum of squares (Residual)

$$SSE = \sum_{i=1}^{n} (y_{data,i} - y_{Model,i})^2 \quad (4)$$

Variation, sum of squares (Regression)

$$SSR = \sum_{i=1}^{n} (y_{Model,i} - \bar{y})^2 \quad (5)$$

$$\bar{y} = \sum_{i=1}^{n} \frac{y_{data,i}}{n} \quad (6)$$

The $n$ is the number of data points.

Variances, MSR (Regression), MSE (Residual), and MS (Total), are the variation divided by the degree of freedom, that is MS = SS/df.

The $F$ statistic is the ratio of two sample variances, $F$ = MSR/MSE, the $t$-ratio is the estimated parameter divided by its standard error, and the $P$-value is the observed significance level of the $F$-ratio or $t$-ratio. The hypotheses were tested at an $\alpha = 0.05$ level.

One measure of performance of a model is its ability to make predictions. In this context, withhold-1 cross-validation of the created models was carried out. In this setting, Allen defined PRESS (predicted sum of squares) as

$$PRESS = \sum_{i=1}^{n} e^2_{(i)} \quad (7)$$

$$RMSEP = \sqrt{\frac{PRESS}{n}} \quad (8)$$

$$q^2_{pre} = 1 - \frac{PRESS}{SSTo} \quad (9)$$

Models with $q^2_{pre} \geqslant 0.6$ can be considered to have good predictive capability.[32]

## 3. Results and discussion

The QSAR study was carried out on selective affinities of a series of substituted imidazoline/oxazoline/guanidine derivatives for [$^{125}$I]*p*-iodoclonidine ([$^{125}$I]PIC) binding to the $\alpha_{2A}$, $\alpha_{2B}$, $\alpha_{2C}$, and $I_1$ receptors.[20] The compounds were evaluated for their binding affinity toward the human $\alpha_{2A}$, $\alpha_{2B}$, and $\alpha_{2C}$ receptors on the transfected CHO (Chinese hamster ovary) cells and $I_1$ receptors on human platelet plasma membranes.[20] Earlier saturation binding experiments were performed with [$^{125}$I]PIC to determine the density ($B_{max}$) of $\alpha_2$-AR expression among the different transfected CHO cell lines and on human platelets $I_1$-R.[7,20]

The rank order of $K_i$ values for this platelet $I_1$-R site[20] was generally consistent with that reported for the binding assays with [$^{125}$I]PIC on PC-12 cell membranes.[33]

The ligands for the QSAR study (Figs. 1 and 3) was selected with an intention of covering a wide range of $I_1$-R and $\alpha_2$-AR affinities,[20] and the negative logarithm of their $K_i$, that is, ($pK_i$) values was calculated.

Previously determined crystal structure of clonidine hydrochloride indicated that the imidazoline part of drug is protonated, and the two nitrogen atoms of the imidazoline moiety are thus chemically equivalent.[18] The selected structural parameters of the experimentally determined structure of clonidine hydrochloride and computed geometries from two DFT methods are listed in Table 1. The optimal geometrical parameters of clonidine computed within B3LYP/6-31+G(d,p)$^{water}$ PCM and B3LYP/3-21G (d,p) method do not considerably differ from those obtained for isolated molecules (Table 1). Therefore, the B3LYP/3–21G (d,p) was selected for geometry optimization of all examined ligands.

An analysis at the B3LYP/3–21G (d,p) level of theory[22,23] optimized species revealed that these are minima since frequency analysis showed that each molecule's Hessian matrix had no negative eigenvalues, thus demonstrating that there were no imaginary frequencies. Earlier B3LYP/6–31+G(d,p) calculations showed, in agreement with experiments, that clonidine and moxonidine exist in a more stable imino tautomer, while rilmenidine amino tautomers being more stable.[15,16]

Calculation of pKa and selection of dominant forms at physiological pH 7.4 were performed for all examined ligands (Fig. 1) using the Marvin 4.0.5 ChemAxon program.[21] Geometries of the most abundant tautomers and isomers of the $I_1$-R ligands at physiological pH (7.4) have been selected and optimized using the Gaussian B3LYP/3–21G (d,p) basis set.[22,23] The optimized models were used for computation of molecular parameters by Gaussian 6-31G(d,p)$^{water}$,[22–26] ChemProp[27] and Marvin 4.0.5 ChemAxon programs.[21]

Among 42 descriptors that were considered in generating the QSAR model, few descriptors such as average partial atomic charges on nitrogens in the heterocyclic moiety (N-charge), logD (pH 7.4), logP, HOMO energy and molar refractivity of the ligands resulted in a statistically significant model.

QSAR model for $I_1$-R binding affinity with the three variables, average partial atomic charge of nitrogens in the heterocyclic moiety (N-charge by B3LYP/6-31G(d,p)$^{water}$ with Mulliken population analysis), logD (pH 7.4) and molar refractivity (MR) of the ligands, $pK_i$ ($I_1$-R) = f (log $D$, N-charge, MR), was developed with the corresponding regression parameters $R^2$ (0.935) and $R^2_{adj}$(0.911). The multivariable model has succeeded the performed cross-validation with $q^2_{pre}$ values 0.803 (Table 2).

The fitting power of the QSAR model may be seen on the plot of predicted vs. observed $pK_i$ values (Fig. 2).

Predictive ability of the generated QSAR model was examined externally by estimating the activities of test molecules moxonidine and guanfacine (**T1** and **T2**, Fig. 3). Their $I_1$-R binding affinity ($pK_i$($I_1$-R)) was determined on human platelets plasma membranes by receptor binding assays with [$^{125}$I] *p*-iodo-clonidine radioligand.[20] Molecular modeling and computation of the molecular parameters of the test compounds was performed by use of the same theoretical procedure.

The root mean square error of estimation (RMSEE) of the two test molecules (RMSEE: 0.877) was less than RMSE of the QSAR models (RMSE: 0.957), so it was concluded that the $pK_i$ ($I_1$-R) = $f$ ($logD_{pH\ 7.4}$, N-charge, MR) linear regression models have good predictive potential.

Furthermore, for recently synthesized series of pyrroline analogs,[33–35] were reported high $I_1$-R/$\alpha_2$-AR selectivity and nanomolar affinity for $I_1$-R. Binding affinity of the pyrroline analog LNP 906 ($K_i$ = 6.03 ± 0.69 nM),[34] determined on PC12 cell membranes ($I_1$-R) by displacement of [$^{125}$I]-PIC specific binding, was in very good agreement with predicted $pK_i$ value by use of the created QSAR model ($K_i$ = 4.12 nM).

**Table 2**
Regression analysis relating the three variables, log*D* at pH 7.4, average partial atomic charges on nitrogens in the heterocyclic moiety (N-charge by B3LYP/6-31G(d,p)$^{water}$ with Mulliken population analysis), and molar refractivity of ligand with experimentally measured ligand binding affinities at human $I_1$-R[20]

| Compound | p$K_i$ ($I_1$-R)[20] | log*D* at pH 7.4 | $N_{avrg}$-charge, B3LYP/6-31(d,p)$^{water}$ | Molar refractivity (MR) [cm$^3$/mole] | $K_i$ ($I_1$-R) [nM ± SEM][20] |
|---|---|---|---|---|---|
| *p*-Iodoclonidine (1) | 8.319 | 3.46 | −0.6207 | 7.1205 | 4.8 ± 1.2 |
| Oxymetazoline (2) | 8.208 | 1.52 | −0.5463 | 7.8620 | 6.2 ± 1.2 |
| Phentolamine (3) | 7.943 | 1.55 | −0.5464 | 8.4232 | 11.4 ± 3.8 |
| Tizanidine (4) | 7.548 | 2.16 | −0.4572 | 6.3976 | 28.3 ± 8.5 |
| Guanabenz (5) | 7.460 | 1.29 | −0.5553 | 6.1750 | 34.7 ± 44.8 |
| Efaroxan (6) | 7.281 | 1.81 | −0.4989 | 6.2935 | 52.4 ± 30.4 |
| Clonidin (7) | 7.260 | 1.07 | −0.6311 | 5.8141 | 55.0 ± 10.0 |
| Rilmenidin (8) | 7.228 | 1.63 | −0.5388 | 5.0763 | 59.2 ± 5.8 |
| Cirazoline (9) | 7.004 | 1.53 | −0.4674 | 6.3335 | 99.0 ± 31.0 |
| Naphazoline (10) | 6.915 | 0.27 | −0.4699 | 6.6144 | 121.6 ± 80.5 |
| BDF, 6143 (11) | 6.635 | −1.02 | −0.6368 | 6.4416 | 232.0 ± 126.0 |
| Idazoxan (12) | 5.901 | 0.90 | −0.1830 | 5.4794 | 1255.0 ± 745.0 |
| *r*, correlation | | 0.653 | −0.620 | 0.666 | |
| Regression equation | | | p$K_i$ ($I_1$-R) = 3.5338 + 0.3527 · log*D* − 2. 6113 · $N_{avrg}$ + 0.3015 · MR | | |
| $R^2$ | | | | | 0.935 |
| $R^2_{adj}$ | | | | | 0.911 |
| RMSE | | | | | 0.957 |
| $q^2_{pre} > 0.6$ | | | | | 0.803 |
| *F*-ratio | | | | | 38.313 |
| *P*-value | | | | | 0.00004 |
| RMSEP | | | | | 0.277 |
| | External validation of the regression model | | | | |
| Compound | p$K_i$ ($I_1$-R) | log*D* at pH 7.4 | $N_{avrg}$-charge, B3LYP/6-31(d,p)$^{water}$ | MR [cm$^3$/mole] | Evaluated p$K_i$ ($I_1$-R) |
| Moxonidin (T1) | 8.377[20] | 1.05 | −0.6250 | 5.9812 | 7.3393 |
| Guanfacine (T2) | 7.721[20] | 1.50 | −0.4452 | 6.0272 | 7.0423 |
| RMSEE | | | | | 0.877 |
| LNP906 | 8.220[33] | 1.93 | −0.6601 | 8.1167 | 8.385 |

RMSEE, root mean square error of estimation; RMSEP, root mean square error of prediction.

Also, good agreement between the observed and evaluated p$K_i$($I_1$-R) values (Fig. 2) and $q^2_{pre}$ value above limit of 0.6 ($q^2_{pre}$ : 0.803) have indicated on high prognostic capability of the multiple linear regression model:

$$pK_i(I_1 - R) = 3.5338 + 0.3527 \cdot \log D_{pH\ 7.4} - 2.6113 \cdot N_{avrg} + 0.3015 \cdot MR$$

The theoretical approach indicates that an increase in distribution coefficient (log*D* at pH 7.4) and molar refractivity value, together with a decrease in average N-charge in the heterocyclic moiety of the ligands, causes better binding affinity for active site of the $I_1$ receptors.

The distribution coefficient (*D*) is the ratio of the sum of the concentrations of all species of the compound in octanol to the sum of the concentrations of all species of the compound in water.

$$D = [\text{Sum of all microspecies}](\text{octanol})/[\text{Sum of all microspecies}](\text{aq})$$
$$\log D = \log_{10}(\text{Distribution Coefficient})$$

The distribution coefficient (log*D*) of a species observed in a water/*n*-octanol system has been adopted as the standard measure of lipophilicity. Thus, higher $\log D_{pH\ 7.4}$ values indicate on increased lipophilic character of the ligands with stronger binding affinity for $I_1$ receptors.

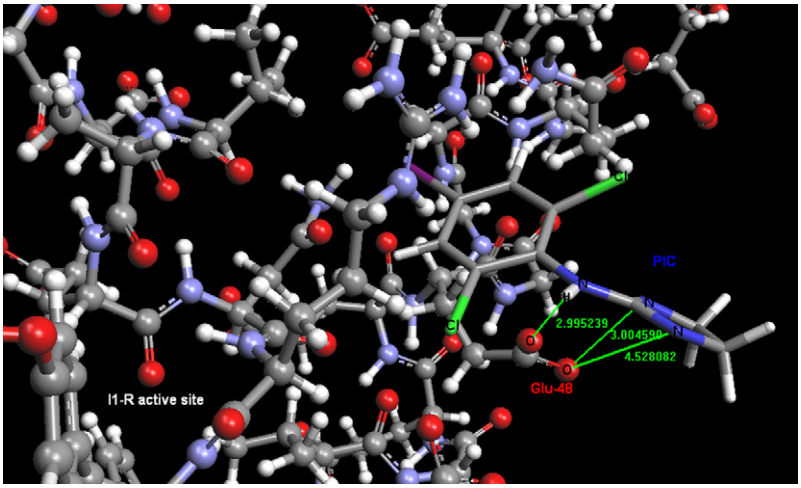


**Figure 4.** Binding mode of the PIC (**1**) into the active domain of the $I_1$-R. The ligand and interacting residues are shown in stick and ball-cylinder representations, respectively. The atoms are shaded by atom type: blue for nitrogen, and red for oxygen.

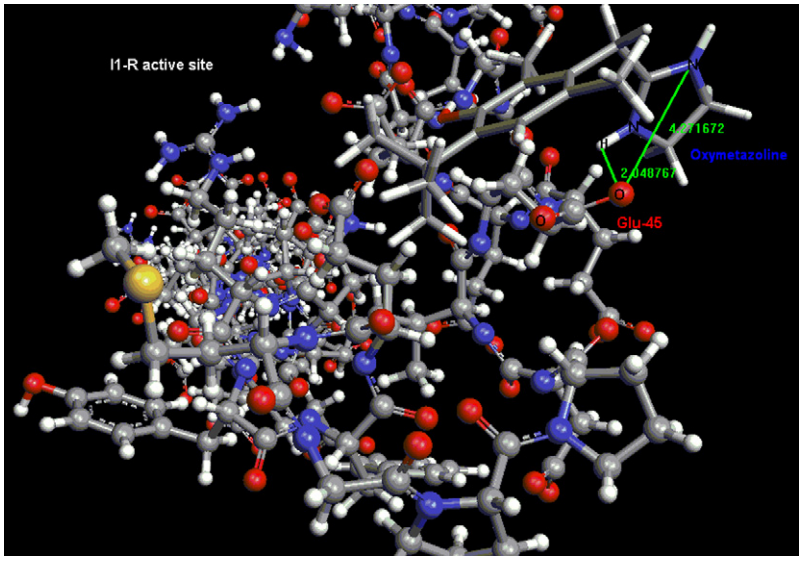


**Figure 5.** Binding mode of the Oxymetazoline (**2**) into the active domain of the $I_1$-R. The ligand and interacting residues are shown in stick and ball-cylinder representations, respectively. The atoms are shaded by atom type: blue for nitrogen, and red for oxygen.

For a radiation of infinite wavelength, the molar refractivity represents the real volume of the molecules. Molar refractivity is related, not only to the volume of the molecules but also to the London dispersive forces that act in the drug-receptor interaction.[36]

The involvement of the both N-atoms in the heterocyclic moiety in the ligands binding on active site of the $I_1$-R was examined by use of the ArgusLab 4.0.1 docking program.[29]

The ArgusLab 4.0.1 docking program[29] has been extensively validated with docking accuracy at ~3 Å, for root mean square deviation (RMSD) value between the predicted and original crystallographic pose.[18] Earlier ArgusLab 4.0.1 validation studies have reported very little difference in the docking accuracies between ArgusLab and Genetic Optimization for Ligand Docking (GOLD).[37,38]

The docking calculation was started with geometry optimization of the active domain of the $I_1$-R, ruthenium binding region (amino acid 629–691),[11] using the UFF method[28] implemented in Argus Lab 4.0.1 (Planaria Software).[29] *p*-Iodoclonidine, as compound with the highest affinity and selectivity for the $I_1$-R ($K_i$: 4.8 nM),[20] has been used for best ligand pose search and selection of the binding amino acids in the active domain of the $I_1$-R (Fig. 4). The *Asp*, *Glu*, *Tyr*, and *Ala* amino acids were identified to form intermolecular bonds with the ligands in the best ligand pose conformation (bond distance less than 4.5 Å). The nitrogen atoms of the heterocyclic moiety of the ligands were always involved in formation of the dipol–dipol interactions with the amino acids in the active domain of the $I_1$-R (Figs. 4 and 5). Furthermore, aromatic moieties of the ligands have created hydrophobic interactions with the amino acids in the active site.

The results of the QSAR model were in good agreement with the docking study of the $I_1$-R ligands. Both studies have indicated on involvement of the N-atoms in the heterocyclic moiety and aromatic parts of the ligands for selective $I_1$-R activation.

Furthermore, selective binding affinities of the ligands to the $\alpha_{2A}$, $\alpha_{2B}$, and $\alpha_{2C}$ receptors[20] were used to calculate average $pK_i(\alpha_2\text{-AR})$ values. The calculated average $pK_i(\alpha_2\text{-AR})$ values were then used for correlation study with the computed molecular parameters of the ligands. HOMO energy of the ligands showed good agreement with the average $pK_i(\alpha_2\text{-AR})$ values (Table 3).

**Table 3**
Regression analysis relating HOMO energy (by B3LYP/6-31G(d,p)$^{water}$ basis set) and partition coefficient octanol/water (log*P*) of the ligands with experimentally measured ligand binding affinities at human $\alpha_2$-AR and $I_1$-R/$\alpha_2$-AR selectivity.[20] RMSEE, root mean square error of estimation; RMSEP, root mean square error of prediction

| Compound | Selectivity, $pK_i(I_1\text{-R})$-$pK_i(\alpha_2\text{-AR})$[20] | $pK_i(\alpha_2\text{-AR})$[20] | HOMO [hartree], B3LYP/6-31(d,p)$^{water}$ | log*P* |
|---|---|---|---|---|
| *p*-Iodoclonidine (1) | −0.1413 | 8.4601 | −0.35355 | 2.743 |
| Oxymetazoline (2) | 1.1837 | 7.0240 | −0.23255 | 4.609 |
| Phentolamine (3) | 0.6992 | 7.2439 | −0.20977 | 3.809 |
| Tizanidine (4) | 0.6197 | 6.9285 | −0.25371 | 2.093 |
| Guanabenz (5) | −1.2540 | 8.7137 | −0.26222 | 2.381 |
| Efaroxan (6) | 0.0996 | 7.1811 | −0.23968 | 2.842 |
| Clonidin (7) | −0.5229 | 7.7825 | −0.26388 | 1.578 |
| Rilmenidin (8) | −0.2875 | 7.5152 | −0.27744 | 1.421 |
| Cirazoline (9) | 0.5891 | 6.4153 | −0.23719 | 2.542 |
| Naphazoline (10) | 0.0827 | 6.8324 | −0.22583 | 3.826 |
| BDF, 6143 (11) | −1.8981 | 8.5326 | −0.25299 | 1.360 |
| Idazoxan (12) | −1.1493 | 7.0506 | −0.24228 | 0.856 |
| *r*, Selectivity-correlation | | | 0.248 | 0.724 |
| *r*, $pK_i(\alpha_2\text{-AR})$-correlation | | | −0.595 | −0.297 |
| Regression equation | Selectivity = $-1.6192 + 0.5805 \cdot \log P$ | | | |
| Regression equation | $pK_i(\alpha_2\text{-AR}) = 4.3731 - 12.1931 \cdot \text{HOMO}$ | | | |

| Compound | Test compounds | | | | | |
|---|---|---|---|---|---|---|
| | Selectivity, $pK_i(I_1\text{-R})$-$pK_i(\alpha_2\text{-AR})$[20] | $pK_i(\alpha_2\text{-AR})$[20] | HOMO [hartree], B3LYP/6-31(d,p)$^{water}$ | log*P* | Selectivity-evaluated | $pK_i(\alpha_2\text{-AR})$-evaluated |
| Moxonidin (T1) | 0.4806 | 7.8962 | −0.25795 | 1.440 | −0.7832 | 7.5184 |
| Guanfacine (T2) | −0.2965 | 8.0177 | −0.26133 | 1.370 | −0.8239 | 7.5596 |

However, it would appear that the HOMO energy of the ligands is important for evaluating their binding affinities to the $\alpha_2$-adrenoreceptors.

Also, inclusion of the compounds lipophilicity in the form of log*P* yields a correlation with $I_1/\alpha_2$-selectivity ($pK_i(I_1\text{-R})$-$pK_i(\alpha_2\text{-AR})$[20] with a correlation factor (*r*: 0.724).

Good agreement between the observed and evaluated $pK_i(\alpha_2\text{-AR})$ and $I_1/\alpha_2$-AR selectivity values have indicated on useful prognostic potential of the derived linear regression equations (Table 3).

## 4. Conclusion

Partial atomic charges of nitrogen in the heterocyclic moiety, $\log D_{\text{pH 7.4}}$, and molar refractivity of the ligands account for the $I_1$-R binding affinities ($pK_i(I_1\text{-R})$). The multiple linear regression models with three variables, $pK_i(I_1\text{-R}) = f\ (\log D_{\text{pH 7.4}}$, N-charge, MR), were developed with the corresponding regression parameter $R^2$ (0.935) and cross-validation parameter of prediction $q^2_{\text{pre}} = 0.803$. Relatively high statistical and validation parameters of the regression model are indicating on its good prognostic capacity.

The proposed QSAR model indicates an increase in lipophilicity ($\log D_{\text{pH 7.4}}$) and molar refractivity, together with a decrease in N-charge in the heterocyclic moiety influence on better affinity for $I_1$ receptors. The performed docking studies have suggested that the N-atoms of the heterocyclic moiety are involved in dipol–dipol interactions between the ligands and the active site of the $I_1$-R.

The described theoretical procedure and derived regression equations could be used for evaluation of binding affinities to the $I_1$-receptors, $\alpha_2$-adrenoreceptors, and $I_1/\alpha_2$-selectivity for the novel ligands.

Since more selective $I_1$ receptor activation can reduce the side effects of $\alpha_2$-adrenoceptors stimulation, the developed QSAR study of $I_1$-R affinity in combination with the QSAR study of the ligands $I_1/\alpha_2$-selectivity can be very helpful for rational design and evaluation of novel selective $I_1$-R ligands with enhanced affinity for $I_1$-receptors.

## Acknowledgment

This work was supported by the Ministry of Science, Technology and Environmental Protection of Serbia, Contract No. 142071.

## Supplementary data

Supplementary data associated with this article can be found, in the online version, at doi:10.1016/j.bmc.2008.06.051.

## References and notes

1. Head, G. A.; Burke, S. L. *J. Hypertens.* **2000**, *18*(9), 1263–1276.
2. Ernsberger, P. *J. Cardiovasc. Pharmacol.* **2000**, *35*, S27–S41.
3. Bousquet, P.; Feldman, J. *Drugs* **1999**, *58*, 799–812.
4. Bock, C.; Niederhoffer, N.; Szabo, B. *Naunyn. Schmiedebergs Arch Pharmacol.* **1999**, *359*, 262–271.
5. Head, G. A.; Mayorov, D. N. *Cardiovasc. Hematol. Agents* **2006**, *4*(1), 17–32.
6. Heemskerk, F. M. J.; Dontenwill, M.; Greney, H.; Vonthron, C.; Bousquet, P. *J. Neurochem.* **1998**, *71*, 2193–2202.
7. Piletz, J. E.; Sletten, K. *J. Pharmacol. Exp. Ther.* **1993**, *267*, 1493–1502.
8. Ernsberger, P.; Graves, M. E.; Graff, L. M.; Zakieh, N.; Nguyen, P.; Collins, L. A. *Ann. N.Y. Acad. Sci.* **1995**, *763*, 22–42.
9. Separovic, D.; Kester, M.; Ernsberger, P. *Mol. Pharmacol.* **1996**, *49*, 668–675.
10. Greney, H.; Ronde, P.; Magnier, C.; Maranca, F.; Rascente, C.; Quaglia, W.; Giannella, M.; Pigini, M.; Brasili, L.; Lugnier, C.; Bousquet, P.; Dontenwill, M. *Mol. Pharm.* **2000**, *57*, 1142–1151.
11. Piletz, J. E.; Ivanov, T. R.; Sharp, J. D., et al *DNA Cell Biol.* **2000**, *19*, 319–329.
12. Piletz, J. E.; Deleersnijder, W.; Roth, B. L.; Ernsberger, P.; Zhu, H.; Ziegler, D. *Ann. N.Y. Acad. Sci.* **2003**, *1009*, 419–426.
13. Lim, K. P.; Hong, W. *J. Biol. Chem.* **2004**, *279*, 54770–54782.
14. Alahari, S. K.; Nasrallah, H. *J. Biochem.* **2004**, *377*, 449–457.
15. Remko, M.; Walshb, O. A.; Richardsb, W. G. *Phys. Chem. Chem. Phys.* **2001**, *3*, 901–907.
16. Remko, M.; Van Duijnen, P. Th.; Swart, M. *Struct. Chem.* **2003**, *14*, 271.
17. Remko, M.; Swart, M.; Bickelhaupt, M. *Bioorg. Med. Chem.* **2006**, *14*, 1715–1728.
18. Byre, G.; Mostad, A.; Rømming, Ch. *Acta Chem. Scand.* **1976**, *B30*, 843.
19. Hu, H. J.; Sun, C. R.; Zhang, H.; Pan, Y. J. *Acta Cryst.* **2005**, *E61*, o413–o415.
20. Piletz, J. E.; Zhu, H.; Chikkala, D. N. *J. Pharmacol. Exp. Ther.* **1996**, *279*, 694–702.
21. Marvin 4.0.5, ChemAxon, Budapest, Hungary. www.chemaxon.com/products.html.
22. Becke, D. *J. Chem. Phys.* **1993**, *98*, 5648.
23. Lee, C.; Yang, W.; Parr, R. G. *Phys. Rev. B* **1988**, *37*, 785.
24. Frisch, M. J.; Trucks, G. W.; Schlegel, H. B.; Scuseria, G. E.; Robb, M. A.; Cheeseman, J. R.; Zakrzewski, V. G.; Montgomery, J. A., Jr.; Stratmann, R. E.; Burant, J. C.; Dapprich, S.; Millam, J. M.; Daniels, A. D.; Kudin, K. N.; Strain, M. C.; Farkas, O.; Tomasi, J.; Barone, V.; Cossi, M.; Cammi, R.; Mennucci, B.; Pomelli, C.; Adamo, C.; Clifford, S.; Ochterski, J.; Petersson, G. A.; Ayala, P. Y.; Cui, Q.; Morokuma, K.; Malick, D. K.; Rabuck, A. D.; Raghavachari, K.; Foresman, J. B.; Cioslowski, J.; Ortiz, J. V.; Baboul, A. G.; Stefanov, B. B.; Liu, G.; Liashenko, A.; Piskorz, P.; Komaromi, I.; Gomperts, R.; Martin, R. L.; Fox, D. J.; Keith, T.; Al-Laham, M. A.; Peng, C. Y.; Nanayakkara, A.; Gonzalez, C.; Challacombe, M.; Gill, P. M. W.; Johnson, B. G.; Chen, W.; Wong, M. W.; Andres, J. L.; Head-Gordon, M.; Replogle, E. S.; Pople, J. A. *Gaussian 98 (Revision A.7)*; Gaussian, Inc.: Pittsburgh PA, 1998.
25. Miertus, S.; Scrocco, E.; Tomasi, J. *Chem. Phys.* **1981**, *55*, 117.
26. Cammi, R.; Tomasi, J. *J. Comput. Chem.* **1995**, *16*, 1449.
27. CS Chem3D Ultra 7.0 (Property Picker ActiveX Control), Cambridge Soft Corporation, 100 Cambridge Park Dr. Cambridge, MA 02140-2317 U.S.A. http://www.cambridgesoft.com/.
28. Casewit, C. J.; Colwell, K. S.; Rappe, A. K. *J. Am. Chem. Soc.* **1992**, *114*, 10035–10046.
29. ArgusLab 4.0, Mark A. Thompson, Planaria Software LLC, Seattle, http://www.ArgusLab.com.
30. Zheng, S.; Chang, C. H.; Ernsberger, P. *J. Neurochem.* **2007**, *101*, 99–108.
31. XNUMBERS, Ver.4.7, March 2006, Multi Precision Floating Point Computing and Numerical Methods for EXCEL/2000 XP.
32. Allen, D. M. *Technometrics* **1974**, *16*, 125.
33. Greney, H.; Urosevic, D.; Schann, S.; Dupuy, L.; Bruban, V.; Ehrhardt, J-D.; Bousquet, P.; Dontenwill, M. *Mol. Pharmacol.* **2002**, *62*, 181–191.
34. Urosevic, D.; Schann, S.; Ehrhardt, J.-D.; Bousquet, P.; Greney, H. *Br. J. Pharmacol.* **2004**, *142*, 609–617.
35. Schann, S.; Bruban, V.; Pompermayer, K.; Feldman, J.; Pfeiffer, B.; Renard, P.; Scalbert, E.; Bousquet, P.; Ehrhardt, J.-D. *J. Med. Chem.* **2001**, *44*, 1588–1593.
36. Gupta, M. K.; Mishra, P.; Prathipati, P.; Saxena, A. K. *Bioorg. Med. Chem.* **2002**, *10*, 3713–3716.
37. Joy, S.; Nair, P. S.; Hariharan, R.; Pillai, M. R. *In Silico Biol.* **2006**, *6*, 0053.
38. Jones, G. ; Willett, P.; Glen, R. C.; Leach, A. R.; Taylor, R. *J. Mol. Biol.* **1997**, *267*, 727–748.